Acta Cryst. (1955). **8**, 394

On the Structures of some Compounds of the Perovskite Type

BY HARRY L. YAKEL, JR.

Oak Ridge National Laboratory, Oak Ridge, Tennessee, U.S.A.

(*Received* 10 *November* 1954 *and in revised form* 11 *January* 1955)

X-ray powder diffraction patterns of a number of compounds and solid solutions of the type ABO_3, where B is a transition metal element, have been recorded and interpreted. These substances all have perovskite-like structures, with characteristic lattice distortions and multiple unit cells which are a result of partial covalent bonding. Variations of structures with differing conditions of preparation are noted for $LaMnO_3$ and $CaMnO_3$, where the results of chemical analyses show that these variations accompany departures from stoichiometric composition. Solid solutions of $LaMnO_3$ and $CaMnO_3$ obey Vegard's rule, a decrease in unit cell volume being produced by the substitution of Ca^{+2} and Mn^{+4} ions in the $LaMnO_3$ structure. An unusual increase in unit cell volume is, however, observed when Sr^{+2} and Co^{+4} ions are substituted in the $LaCoO_3$ structure.

Introduction

Current crystallographic interest in compounds of the type ABO_3, which have structures closely related to the so-called perovskite structure, stems from the unusual physical properties of these substances (Megaw, 1952, 1954). While a complete description of the small atomic displacements responsible for the pseudo-symmetric structures so often found in such compounds seems to require single-crystal diffraction data (Evans, 1951; Vousden, 1951*b*, 1954), much useful information can be derived from the unit-cell dimensions and apparent lattice symmetries observed in powder diffraction experiments (Vousden, 1951*a*).

It is the purpose of this paper to describe and discuss the X-ray powder diffraction data obtained for a group of compounds of the perovskite type whose neutron diffraction patterns at liquid helium temperatures indicate the presence of several interesting ferromagnetic and antiferromagnetic structures (Jonker & van Santen, 1950; Wollan & Koehler, to be published). All of the X-ray experiments were performed at room temperatures, but it was hoped that they would provide some clues to the behavior of the compounds at low temperatures.

Experimental

The compounds included in the present investigation were* $LaMnO_3$, $CaMnO_3$, $LaCoO_3$, $SrCoO_3$, $LaFeO_3$, $SrFeO_3$, $LaCrO_3$ and $LaVO_3$. Some solid solutions of the type $(La_xCa_{1-x})MnO_3$, $(La_xSr_{1-x})CoO_3$, etc., were also studied. Pure compounds and solid solutions were prepared from stoichiometric amounts of the appropriate oxides, hydroxides, or carbonates by firing at temperatures in excess of 1000°C. in atmospheres ranging from pure oxygen to 99% N_2–1% O_2 for periods of 2–25 hr. The samples were quenched from firing temperatures to room temperature. Chemical analyses for tetrapositive transition metal ions were made as a check on the purity of the compound preparations and on the accuracy of the nominal solid-solution compositions.* As an example of the effects of varying temperatures and atmospheres on the resultant preparations, it was found that $LaMnO_3$ samples prepared at temperatures of 1100–1400° C. in air or nitrogen atmospheres, with long firing periods, contain about 8–10% of the manganese as Mn^{+4}, while samples of the same substance prepared at 1000° C. in pure oxygen, with short firing times, contain as much as 35% Mn^{+4}. The ease with which such variations from ideal composition can be introduced into compounds having perovskite-like structures has frequently been noted (Wells, 1945).

Attempts to prepare sizable single crystals of these compounds were not successful, so that powder diffraction techniques alone could be used. A 57·3 mm. radius Debye–Scherrer camera of standard design was employed for photographic measurements and a Norelco high-angle X-ray goniometer was used in

---

* These are nominal, not necessarily actual, formulae.

* The analyses for tetrapositive transition metal ions were carried out in two steps. The first involved a determination of the total oxidizing power of the sample, and the second a determination of the total transition metal concentration. Together these results gave values for the tri- and tetrapositive ion content which are probably accurate to ∓5%.

As an example, in an analysis for Mn^{+3} and Mn^{+4}, part of the sample was dissolved in a known excess of standard ferrous sulfate solution. The excess Fe^{+2} was then titrated with standard potassium permanganate solution and the number of milliequivalents of iron oxidized by Mn^{+3} and Mn^{+4} was obtained by the difference between the total milliequivalents of Fe^{+2} added and the milliequivalents of excess iron determined by titration. The remainder of the sample was analyzed for total manganese by dissolution in nitric acid and hydrogen peroxide, followed by oxidation of the manganese to permanganate by sodium bismuthate. A known volume of standard ferrous sulfate solution was added to the permanganate and the excess Fe^{+2} was titrated with standard potassium permanganate solution. The analyses for cobalt, iron and chromium were performed by similar methods.

Table 1

Nominal formula	B^{+4} (%)	a (Å)	b (Å)	c (Å)	β or α	V (Å^3)	Symmetry§	Previous investigation
$LaMnO_3$	8·9	7·960†	7·698	7·960	91° 52′	487·5	*M*	Cubic, a = 3·88 Å (Náray-Szabo, 1943)
		11·439*	7·698	11·072	—	—	*O*	
$LaMnO_3$	25·4	7·812†	7·794	7·812	90° 13′	475·6	*M*	
		11·069	7·794	11·027	—	—	*O*	
$LaMnO_3$	35·3	7·769	—	—	90° 35′	468·8	*R*	
$La_{0{\cdot}93}Ca_{0{\cdot}07}MnO_3$	—	7·909†	7·708	7·909	91° 26′	482·0	*M*	
		11·324	7·708	11·044	—	—	*O*	
$La_{0{\cdot}85}Ca_{0{\cdot}15}MnO_3$	18·5	7·848†	7·734	7·848	90° 45′	476·3	*M*	
		11·171	7·734	11·026	—	—	*O*	
$La_{0{\cdot}75}Ca_{0{\cdot}25}MnO_3$	30·5	7·772	—	—	—	469·1	**	
$La_{0{\cdot}60}Ca_{0{\cdot}40}MnO_3$	43·5	7·710	—	7·677	—	456·4	*T*	
$La_{0{\cdot}50}Ca_{0{\cdot}50}MnO_3$	49·4	7·697	—	—	—	456·0	*C*	
$La_{0{\cdot}50}Ca_{0{\cdot}50}MnO_3$	56·4	7·689†	7·675	7·689	90° 7′	453·8	*M*	
		10·884	7·675	10·864	—	—	*O*	
$La_{0{\cdot}40}Ca_{0{\cdot}60}MnO_3$	71·2	7·628	—	7·584	—	441·3	*T*	
$La_{0{\cdot}25}Ca_{0{\cdot}75}MnO_3$	78·5	7·568	—	—	—	433·5	*C*	
$CaMnO_3$	71·0	7·481†	7·449	7·481	91° 7′	416·8	*M*	Distorted cubic, a = 3·73 Å for 80% Mn^{+4} (Jonker & Van Santen, 1950)
		10·683	7·449	10·476	—	—	*O*	
$CaMnO_3$	90·8	7·465	—	—	—	416·0	*C*	
$CaMnO_3$	96·9	7·465	—	—	—	416·0	*C*	
$LaFeO_3$	5·0	7·852	—	—	—	484·1	*C*	Cubic, a = 3·89 Å (Náray-Szabo, 1943)
$SrFeO_3$	86·1	3·869	—	—	—	463·3‡	*C*	
$LaCoO_3$	—	7·651	—	—	90° 40′	447·8	*R*	Rhombohedral, a = 3·82 Å, α = 90° 40′ (Askham *et al.*, 1950)
$La_{0{\cdot}80}Sr_{0{\cdot}20}CoO_3$	34·1	7·658	—	—	90° 30′	449·1	*R*	
$La_{0{\cdot}65}Sr_{0{\cdot}35}CoO_3$	—	7·664	—	—	90° 23′	450·1	*R*	
$La_{0{\cdot}50}Sr_{0{\cdot}50}CoO_3$	—	7·668	—	—	—	450·9	*C*	
$SrCoO_3$	1·4	7·725	—	—	—	461·0	*C*	
$LaCrO_3$	3·8	7·777†	7·750	7·777	90° 15′	467·1	*M*	Cubic, a = 3·88 Å (Náray-Szabo, 1943)
		11·022	7·750	10·975	—	—	*O*	Cubic, a = 3·90 Å (Wold & Ward, 1954)
$La_{0{\cdot}50}Sr_{0{\cdot}50}CrO_3$	—	7·754	—	—	—	466·2	*C*	
$SrCrO_3$	—	—	—	—	—	—	††	
$LaVO_3$	—	7·842	—	—	—	482·3	*C*	Cubic, a = 3·91 Å (Wold & Ward, 1954)

* Since the *B*-face of the monoclinic unit cell is a rhombus, an orthorhombic cell defined by the *B*-face diagonals and the *b* axis of the monoclinic cell can also be chosen. For purposes of discussion, it is frequently convenient to use the monoclinic rather than the orthorhombic cell since its axes correspond with those of the undistorted perovskite cube. The true lattice symmetry would, of course, have to be determined from single-crystal data.

† But for a few very weak reflections, the unit cell defined by these monoclinic parameters would be *B*-face centered. Therefore, if these reflections are neglected, the corresponding orthorhombic unit cell would be defined by *a* and *c* axes of half the length given in this table.

‡ The volume of a cell with doubled edges is given here for purposes of comparison only.

§ *M*: monoclinic; *O*: orthorhombic; *R*: rhombohedral; *T*: tetragonal; *C*: cubic.

** Unmeasurable: monoclinic–orthorhombic splitting.

†† Structure unrelated to perovskite.

spectrometer work. Radiations appropriate for the substance studied were used throughout.

Results

The diffraction patterns of all the compounds and solid solutions enumerated above are closely related to the patterns which would be expected from simple perovskite structures (Goldschmidt, 1926*a*, *b*). Differences between the ideal and observed patterns are the split reflections and superlattice reflections shown in the latter, which imply distortions of the lattice from cubic symmetry and an ordering of the atomic displacements and/or of the defects responsible for these distortions.

As shown by Megaw (1946*a*), the number and intensity of the diffraction lines into which a given cubic perovskite reflection is split by distortion of the unit cube are quite different depending on the nature of the distortion. Thus, except in cases where the splitting is so very slight as to make the separate reflections all but indistinguishable, the assignment of probable lattice symmetry and the indexing of the pattern is not difficult. The measured unit-cell parameters and lattice symmetries of the compounds and solid solutions studied are presented in Table 1. Wherever possible, the results of chemical analyses for tetrapositive transition metal ions are listed. Some of the compounds included in the present investigation have been examined previously, and in these cases results of the earlier investigations are also given.

It must be remembered that, since the materials studied were available only as powders, the diffraction patterns obtained therefrom may indicate a higher lattice symmetry than the true one.

Ionic radii

In the analysis of the results listed in Table 1, it is convenient to introduce ionic radii, which, while often representing a rather artificial concept, are nevertheless useful relative reference points for the discussion. For the non-transition metal ions, the crystal radii given by Pauling (1945, p. 346) are used. When available, empirical crystal radii of the transition metal ions have been assumed (Pauling, 1945, p. 350). In the case of the Mn^{+4} ion, Goldschmidt's (1926*a*, *b*) value for the radius has been used, while for ions such as Cr^{+4}, Fe^{+4}, Co^{+3} and Co^{+4}, for which radii have not been given, an attempt has been made to interpolate a set of values which will be consistent with the empirical radii of other ions of the transition group. The curves used in this interpolation are shown in Fig. 1. A list of the radii to be employed in the following section is given in Table 2.

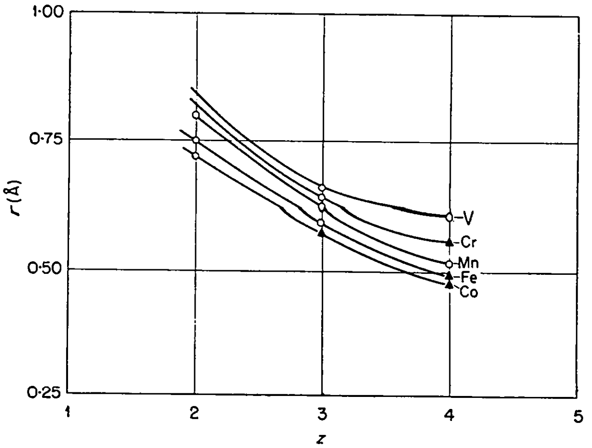

Fig. 1. Ionic radii of transition metal ions of the third row as a function of their nuclear charge, *z*. Circles: empirical radii; triangles: interpolated radii.

Table 2. *Ionic radii*

Ion	Radius (Å)	Ion	Radius (Å)
O^{-2}	1·40	Cr^{+4}	0·56
Ca^{+2}	1·08*	Mn^{+3}	0·62
Sr^{+2}	1·22*	Mn^{+4}	0·52
La^{+3}	1·22*	Fe^{+3}	0·60
V^{+3}	0·66	Fe^{+4}	0·50
V^{+4}	0·61	Co^{+3}	0·58
Cr^{+3}	0·64	Co^{+4}	0·48

* Corrected for change from 6-fold to 12-fold coordination (Pauling, 1945, p. 368).

Discussion

The ideal perovskite structure for compounds of the type ABO_3 may be described as cubic, with 12-fold coordinated *A* ions at the corners, 6-fold coordinated *B* ions at the body centers, and 6-fold coordinated O ions at the face centers of the unit cubes. In the series of structures reported here, the transition metal ions correspond to the octahedrally coordinated *B* ions.

Since the departures from cubic symmetry exhibited by the compound included in Table 1 are, in general, small, reasonable average values for interionic distances can be calculated from the equations

$$r_{O-B} = \tfrac{1}{4}V^{\frac{1}{3}}, \quad (1)$$

$$r_{O-A} = r_{O-O} = \tfrac{1}{4}\sqrt{2}\,.\,V^{\frac{1}{3}}, \quad (2)$$

where V is the volume of the unit cell. Table 3 presents these distances together with the radius sums calculated from Table 2, and the differences, δ, between theoretical and observed distances. Tolerance factors, t, which are a measure of the degree of misfit of the structure, can be defined by the equation

$$(R_O+R_A) = \sqrt{2}\,.\,t(R_O+R_B)\,, \quad (3)$$

where R_O, R_A, and R_B are theoretical ionic radii (Goldschmidt, 1926*a*, *b*). Values of this factor are also given in Table 3.

The negative δ values of Table 3 indicate comparatively small interionic distances between oxygen ions and between oxygen and transition metal ions. These negative δ's probably reflect partial covalent bond

Table 3

Compound	$(\mathrm{O}-B)_{\mathrm{obs.}}$ (Å)	$R_{\mathrm{O}}+R_B$ (Å)	δ_1 (Å)	$(\mathrm{O}-A)_{\mathrm{obs.}}$ (Å)	$R_{\mathrm{O}}+R_A$ (Å)	δ_2 (Å)	t
$LaVO_3$	1·96	2·06	−0·10	2·77	2·62	+0·15	0·90
$SrVO_3$	—	2·01	—	—	2·62	—	0·92
$LaCrO_3$	1·94	2·04	−0·10	2·74	2·62	+0·12	0·91
$SrCrO_3$	—	1·96	—	—	2·62	—	0·95
$LaMnO_3$	1·98	2·02	−0·04	2·79	2·62	+0·17	0·92
$CaMnO_3$	1·87	1·92	−0·05	2·64	2·48	+0·16	0·92
$LaFeO_3$	1·96	2·00	−0·04	2·78	2·62	+0·16	0·93
$SrFeO_3$	1·94	1·90	+0·04	2·74	2·62	+0·12	0·98
$LaCoO_3$	1·91	1·98	−0·07	2·71	2·62	+0·09	0·94
$SrCoO_3$	1·93	1·88	+0·05	2·73	2·62	+0·11	0·98

$$\delta_1 = (\mathrm{O}-B)_{\mathrm{obs.}} - (R_{\mathrm{O}}+R_B)$$
$$\delta_2 = (\mathrm{O}-A)_{\mathrm{obs.}} - (R_{\mathrm{O}}+R_A)$$

character (Vousden, 1951*a*), but any quantitative conclusions are precluded by the uncertainties in the ionic radii. The small positive values of δ_1 obtained for $SrFeO_3$ and $SrCoO_3$ may also be due to inaccurate radii, or to the non-stoichiometric composition of these substances. This latter effect should be especially important for the cobalt compound where the analytical data for Table 1 suggests that the structure actually contains trivalent cobalt ions and random defects arranged on a perovskite lattice. The nature of these defects may be either (*a*) anion holes, giving a composition $SrCoO_{2{\cdot}5}$, (*b*) interstitial cations, giving a composition $Sr_{1{\cdot}5}CoO_3$, or (*c*) anion holes and a disordered array of Sr^{+2} and Co^{+3} ions occupying the *B*-ion sites. A composition corresponding to this latter defect would be $Sr(Co_{0{\cdot}8}Sr_{0{\cdot}2})O_{2{\cdot}4}$. The fact that the lattice parameter for the strontium-cobalt oxide is significantly larger than the average parameter of $LaCoO_3$, together with the nearly equal sizes of the La^{+3} and and Sr^{+2} ion, seems to favor possibility (*b*) or (*c*), but the increased partial covalent bonding in the lanthanum compound may more than account for the observed differences. Since interstitial cations are not likely in the perovskite lattice and there is little precedent for a defect of the (*c*) type, the situation is unresolved.

Megaw (1946*b*) has found that the different possible distortions of perovskite structures from cubic symmetry occur for separate ranges of values of the tolerance factor. Thus, with Goldschmidt's (1926*a*, *b*) ionic radii, $0{\cdot}8 < t < 0{\cdot}9$ should lead to orthorhombic (monoclinic) structures, whereas $0{\cdot}9 < t < 0{\cdot}97$ should lead to cubic symmetry and $0{\cdot}97 < t < 1{\cdot}02$ to tetragonal symmetry. It is seen that the tolerance factors for the compounds listed in Table 3, while not directly comparable to Megaw's owing to the use of Pauling's radii, cannot be grouped in any such consistent sequence. It would seem, therefore, that factors other than relative radii, such as the degree of covalent character in the bonds between the transition metal atom and the surrounding oxygen atoms (Megaw, 1947), may play an important role in determining the atomic displacements and, through them, the lattice symmetry.

The possibility of partial covalent bonding, indicated by small interatomic distances and by the lattice distortions, gives some explanation of the ferromagnetic and antiferromagnetic properties observed in these compounds at low temperatures. Indeed, a magnetic coupling between the transition metal atoms would be difficult to explain if the bonds between these atoms and the intervening oxygen atoms did not have considerable covalent character. A more detailed description of the application of the crystallographic results to the magnetic observations at low temperatures will appear shortly (Wollan & Koehler, to be published).

The doubled perovskite unit cell edges so frequently recorded in Table 1 suggest puckered structures, with antiparallel atomic displacements, as found by Vousden (1951*b*) in $NaNbO_3$. These structures are therefore not likely to be ferroelectric unless a metastable ferroelectric structure can be induced by an applied field (Megaw, 1952).

Of the solid solution systems studied, the $(La_xSr_{1-x})CoO_3$ system, at low Co^{+4} ion concentrations presents the interesting example of a lattice which expands on the substitution of supposedly smaller Co^{+4} ions for Co^{+3} ions and Sr^{+2} ions for La^{+3} ions, the latter pair being of about the same size. A possible explanation for this effect may lie in the fact that the percentage charge decrease at the *A*-ion sites is greater in magnitude than the percentage charge increase at the *B*-ion sites. This might lead to a net decrease in the partial covalent character of the bonds involving oxygen ions and so to the observed lattice expansion.

On the other hand, the $(La_xCa_{1-x})MnO_3$ system shows a continuous linear decrease of lattice volume with increasing Mn^{+4} content (see Fig. 2).* The contraction is in qualitative agreement with the expected decrease in transition-metal ion size, but does not reflect the net decrease in covalent bond character accompanying the substitution of Ca^{+2} ions for La^{+3} ions. This is presumably due to the significantly smaller size of the Ca^{+2} ion, in comparison with the La^{+3} ion, which offsets any expansion of the structure.

---

* For effect of the size of the *A* ion on this solubility, compare this result with those reported for the $LaMnO_3$–$SrMnO_3$ system by Harwood (1954).

As shown in Fig. 2, the unit-cell volumes of calcium manganate (IV) samples containing differing amounts of Mn^{+4} (71–98%, depending on the method of preparation) do not vary significantly. Substitution of trivalent ions for some tetravalent manganese ions should lead to an expansion of the ideal $CaMnO_3$ lattice, but charge equality demands that this substitution be accompanied by the introduction of either interstitial cations or anion vacancies. In order to explain the observed results, the vacancy model must be adopted, since this would lead to a lattice shrinkage which would compensate for the aforementioned expansion.

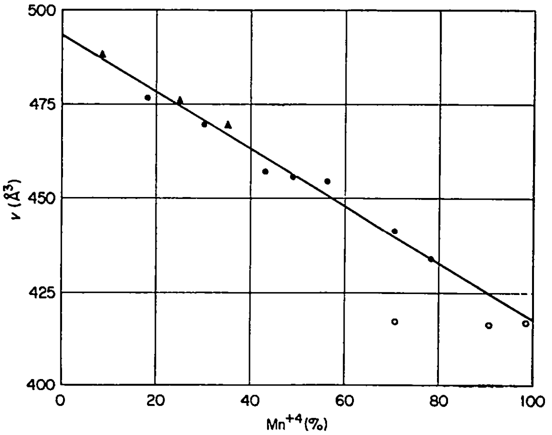

Fig. 2. Unit-cell volume as a function of Mn^{+4} concentration for the solid solution system ($LaMnO_3$–$CaMnO_3$) (solid circles). Open circles represent calcium manganate (IV) samples and triangles represent lanthanum manganate (III) samples prepared under different experimental conditions.

On the other hand, substitution of Mn^{+4} ions for some Mn^{+3} ions in the ideal $LaMnO_3$ structure should lead to lattice shrinkage due to the smaller size of the tetravalent ion, and to either interstitial anions or cation vacancies. Again a vacancy model must be adopted to explain the observations. However, in this case the lattice vacancies do not seem to contribute significantly to the shrinkage, as is shown by the fact that the cell volumes for $LaMnO_3$ defect structures follow the same straight line as the solid solutions of $CaMnO_3$ in $LaMnO_3$ where, of course, no defects should occur.

The above deductions are somewhat idealized in that the observed distortions from the ideal perovskite structure are ignored. Presumably the atomic displacements responsible for the distortions are not large enough to affect the situation significantly.

It is difficult to assess the importance of the differences between the results of the present investigation and those previous results included in Table 1. In most cases, these differences depend on weak reflections, indicative of multiple cells which might be overlooked on weaker diffraction photographs. In one or two cases, however, split reflections due to previously unreported lattice distortions have been found. A possible explanation of this effect may lie in the wide variability of structure characteristic of these substances when prepared under different conditions.

The author wishes to thank Dr E. O. Wollan and Dr W. C. Koehler for their encouragement and many helpful discussions in connection with this work. Thanks are also due to Mr D. E. LaValle, who prepared many of the samples studied, Mr A. D. Horton, who performed the chemical analyses of the samples, and Mr R. M. Steele, whose assistance in recording the X-ray data was most helpful.

References

Askham, F., Fankuchen, I. & Ward, R. (1950). *J. Amer. Chem. Soc.* **72**, 3799.

Evans, H. T. (1951). *Acta Cryst.* **4**, 377.

Goldschmidt, V. M. (1926*a*). *Skr. norske Vidensk. Akad.* No. 2.

Goldschmidt, V. M. (1926*b*). *Skr. norske Vidensk. Akad.* No. 8.

Harwood, M. G. (1954). Paper No. 25, § 5, presented before the Third International Congress of the International Union of Crystallography, Paris (see *Acta Cryst.* (1954), **7**, 641).

Jonker, G. H. & Santen, J. H. van (1950). *Physica*, **16**, 337.

Megaw, H. D. (1946*a*). *Proc. Phys. Soc.* **58**, 133.

Megaw, H. D. (1946*b*). *Trans. Faraday Soc.* A, **42**, 224.

Megaw, H. D. (1947). *Proc. Roy. Soc.* A, **189**, 261.

Megaw, H. D. (1952). *Acta Cryst.* **5**, 739.

Megaw, H. D. (1954). *Acta Cryst.* **7**, 187.

Náray-Szabo (1943). *Naturwissenschaften*, **31**, 466.

Pauling, L. (1945). *The Nature of the Chemical Bond*, 2nd ed. Ithaca: Cornell University Press.

Vousden, P. (1951*a*). *Acta Cryst.* **4**, 373.

Vousden, P. (1951*b*). *Acta Cryst.* **4**, 545.

Vousden, P. (1954). *Acta Cryst.* **7**, 321.

Wells, A. F. (1945). *Structural Inorganic Chemistry*, p. 331. Oxford: Clarendon Press.

Wold, A. & Ward, R. (1954). *J. Amer. Chem. Soc.* **76**, 1029.

Wollan, E. O. & Koehler, W. C. To be published.